PROCEEDINGS - 37th ANNUAL CONDENSED MATTER AND MATERIALS MEETING, 5 - 8 February, 2013. Wagga Wagga, NSW, Australia

Exploiting Fitted Electric Field Gradient Parameters: Axis Ambiguity and the Asymmetry Parameter Constraint, $0 \leq \eta \leq 1$

G.A. Stewart

School of Physical, Environmental and Mathematical Sciences, UNSW Canberra, Australian Defence Force Academy, PO Box 7916, Canberra BC 2610.

Electric field gradient results derived from experimental nuclear quadrupole interaction data can appear deceptively straightforward. This paper explains the connection between the conventional frame (for which the asymmetry parameter lies between zero and unity) and its five perturbations. Consequences are illustrated through two case studies.

1. Introduction

In experimental hyperfine interaction techniques such as nuclear magnetic resonance and Mössbauer spectroscopy, it is common to fit the quadrupole interaction in terms of the electric field gradient (efg), $V_{ZZ} = \partial^2 V/\partial Z^2$, and the asymmetry parameter,

$$\eta = (V_{XX} - V_{YY})/V_{ZZ} \quad (1)$$

where η is constrained to lie within the range $0 \leq \eta \leq 1$. Implicit in this approach are two assumptions:

(i) *The axes, X, Y and Z, are the principal efg axes*. That is, when expressed with respect to this particular spatial alignment of axes, the 3 x 3 efg tensor is diagonalised.

(ii) *The principal efg axes are labelled to give* $|V_{ZZ}| \geq |V_{YY}| \geq |V_{XX}|$. It is only when this convention is satisfied that $0 \leq \eta \leq 1$. This frame will be referred to as the *conventional* frame.

How well the implicit axes are known depends on the local site symmetry of the probe atom. In the case of hexagonal, trigonal or tetragonal symmetries, the situation is clear. The principal Z-axis is the only axis of importance ($\eta = 0$) and it is aligned with the local symmetry axis. For orthorhombic symmetry, the three principal axes are aligned with the local 2-fold symmetry axes but the labelling that is consistent with $0 \leq \eta \leq 1$ is unknown. For lower symmetries, the spatial alignment of at least two of the three principal axes is also unknown, providing a complication further to the axis labelling ambiguity. Unless additional experimental information or theoretical calculations can be drawn on to resolve these issues, care must be taken when exploiting the fitted V_{ZZ} and η values in an alternative frame of reference.

2. The asymmetry parameter in alternative (non-conventional) frames

Bearing in mind that the efg tensor components are not influenced by axis sense, there are only 6 ways that the principal axes can be labelled (Fig. 1). The upper three coordinate frames in Fig. 1 represent the conventional frame, X Y Z, and its two cyclic permutations. The lower frames are generated from the upper frames by a simple rotation through $\pi/2$ about the Z′ axis. By combining Laplace's equation and the definition of the asymmetry parameter,

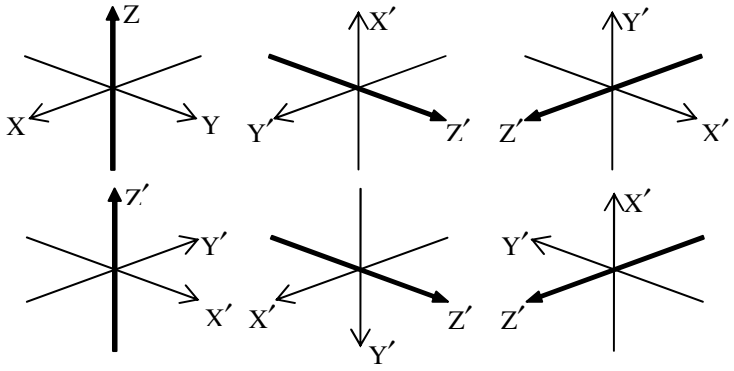

Fig. 1. Alternative axis labels for the same set of principal efg axes. The conventional frame (top left) is assumed to be labelled such that $|V_{ZZ}| \geq |V_{YY}| \geq |V_{XX}|$ with $0 \leq \eta \leq 1$.

it is straightforward to solve for the individual principal efg values in the conventional frame:

$$\left.\begin{array}{lcl} V_{XX} + V_{YY} + V_{ZZ} = 0 & \rightarrow & V_{XX} + V_{YY} = -V_{ZZ} \\ \eta = (V_{XX} - V_{YY})/V_{ZZ} & \rightarrow & V_{XX} - V_{YY} = \eta\, V_{ZZ} \end{array}\right\} \rightarrow \boxed{\begin{array}{lcl} V_{XX} & = & +\tfrac{1}{2}(\eta-1)\, V_{ZZ} \\ V_{YY} & = & -\tfrac{1}{2}(\eta+1)\, V_{ZZ} \\ V_{ZZ} & = & V_{ZZ} \end{array}} \qquad (2)$$

The left hand sides of the boxed expressions in (2) can then be relabelled as required and the $V_{Z'Z'}$ and η' expressions derived for the five alternative frames in terms of V_{ZZ} and η for the conventional frame. The resulting expressions are summarised in Table 1 and the values of η' are presented in Fig. 2 as a function of $0 \leq \eta \leq 1$ for the conventional frame. Based on the results provided in Table 1 and Fig. 2, it is observed that

(i) There is no constraint on the value of η' that might be calculated with respect to an arbitrary set of principal efg axes. It can range over all values from -∞ to +∞. However, the range that the calculated value falls into points to the relative orientation of the conventional frame via Fig. 2 coupled with Fig. 1.

(ii) As a special case, the calculated value of $\eta' = +3$ (–3) implies that $\eta = 0$ in the conventional frame with Z // Y′ (X′) as its symmetry axis.

(iii) The situations for the upper and lower coordinate frames shown in Fig. 1 differ only with respect to the sign of η'. That is, a coordinate rotation through $\pi/2$ about the Z′ axis serves only to change the sign of η'.

Table 1. Electric field gradient $V_{Z'Z'}$ and asymmetry parameter η' expressed in terms of their conventional frame values. The Euler angles α, β, γ correspond to the transformation from the conventional frame to the alternative frames (shown in Fig. 1).

X Y Z //	X′ Y′ Z′	-Y′ X′ Z′	Y′ Z′ X′	X′ Z′ –Y′	Z′ X′ Y′	Z′ -Y′ X′
α, β, γ	0, 0, 0	$0, 0, \frac{\pi}{2}$	$-\frac{\pi}{2}, -\frac{\pi}{2}, 0$	$-\frac{\pi}{2}, -\frac{\pi}{2}, \frac{\pi}{2}$	$0, \frac{\pi}{2}, \frac{\pi}{2}$	$0, \frac{\pi}{2}, \pi$
$V_{Z'Z'}/V_{ZZ}$	1	1	$-\frac{1}{2}(\eta+1)$	$-\frac{1}{2}(\eta+1)$	$\frac{1}{2}(\eta-1)$	$\frac{1}{2}(\eta-1)$
η'	η	$-\eta$	$\left(\frac{\eta-3}{\eta+1}\right)$	$-\left(\frac{\eta-3}{\eta+1}\right)$	$-\left(\frac{\eta+3}{\eta-1}\right)$	$\left(\frac{\eta+3}{\eta-1}\right)$

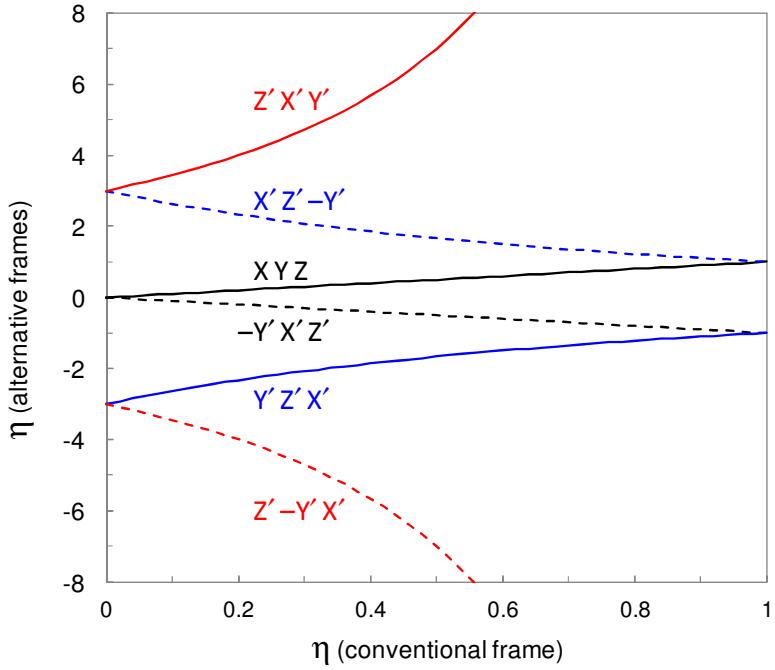

Fig. 2. The electric field gradient asymmetry parameter, η', for alternative frames is plotted as a function of its value in the conventional frame (for which $|V_{ZZ}| \geq |V_{YY}| \geq |V_{XX}|$ and $0 \leq \eta \leq 1$).

3. Applications in rare earth crystal field theory

The perturbative crystal field (CF) interaction of the local charge distribution with a rare earth ion's 4f shell is commonly represented as a multipole expansion of Stevens operator equivalents [1], $O_n^m(J)$,

$$\mathcal{H}_{CF} = \sum_{m=-2}^{+2} B_2^m O_2^m(J) + \sum_{m=-4}^{+4} B_4^m O_4^m(J) + \sum_{m=-6}^{+6} B_6^m O_6^m(J) \qquad (3)$$

and its characterization is then reduced to a matter of determining the sometimes considerable number of CF parameters B_n^m. A useful semi-empirical approach is to use

(i) theoretical calculations to estimate the higher rank ratios $r_4^m = B_4^m/B_4^0$ and $r_6^m = B_6^m/B_6^0$ so that only B_4^0 and B_6^0 need to be determined (fitted) independently, and

(ii) experimental quadrupole interaction determinations of the lattice efg components to estimate the rank 2 CF parameters

$$B_2^0 \propto V_{ZZ}^{latt} \quad \text{and} \quad B_2^2 = \eta^{latt} B_2^0 \qquad (4)$$

with respect to the conventional efg frame.

However, as emphasised in section 2, it is necessary to allow for the possibility that the axes implicit in (ii) may not align with those used for the theoretical calculation in (i).

3.1 Interpretation of inelastic neutron scattering results for intermetallic $ErNiAl_4$

In this recent example [2], cold source neutron inelastic neutron scattering (INS) was employed to determine the first three excited levels of the CF scheme for the single Er^{3+} site in $ErNiAl_4$ and then the semi-empirical approach described above was used to fit a preliminary set of CF parameters. For the orthorhombic C_{2v} (mm) site symmetry, the CF

Hamiltonian simplifies to

$$\mathcal{H}_{CF} = B_2^0O_2^0 + B_2^2O_2^2 + B_4^0O_4^0 + B_4^2O_4^2 + B_4^4O_4^4 + B_6^0O_6^0 + B_6^2O_6^2 + B_6^4O_6^4 + B_6^6O_6^6 \qquad (5)$$

as long as the coordinate axes X′ Y′ Z′ are chosen to align with the 2-fold symmetry axes (in this case, the crystallographic axes). Point charge model values of the higher rank ratios r_4^m and r_6^m were therefore calculated with respect to X′ Y′ Z′ // a b c. Experimental ^{155}Gd-Mössbauer results published earlier for isostructural $GdNiAl_4$ provided estimates of V_{ZZ}^{latt} and η^{latt} for the implicit conventional efg frame X Y Z. However, because of the labelling ambiguity described in Fig. 1, six possible sets of B_2^0 and B_2^2 were estimated using Table 1 and equation (4). Independent B_4^0/ B_6^0 grid searches were conducted for all 6 scenarios and the best set of CF parameters was found to correspond to X Y Z // a –c b. Planned thermal source neutron INS measurements should result in a further refinement of the set of CF parameters.

3.2 Analysis of ^{169}Tm-Mössbauer results for the "green phase" cuprate Tm_2BaCuO_5

In this second example [3], ^{169}Tm-Mössbauer spectroscopy was employed to monitor the temperature-dependent nuclear quadrupole splitting at the two Tm-sites of Tm_2BaCuO_5 (space group Pnma). A semi-empirical approach similar to that described for $ErNiAl_4$ in section 3.1 was then used to fit sets of CF parameters to the experimental data. However, the monoclinic C_s (m) site symmetry introduces an additional ambiguity. The CF Hamiltonian simplifies to

$$\mathcal{H}_{CF} = B_2^0O_2^0 + B_2^2O_2^2 + B_2^{-2}O_2^{-2} + B_4^0O_4^0 + B_4^2O_4^2 + B_4^{-2}O_4^{-2} + B_4^4O_4^4 + B_4^{-4}O_4^{-4} + B_6^0O_6^0 + B_6^2O_6^2 + B_6^{-2}O_6^{-2} + B_6^4O_6^4 + B_6^{-4}O_6^{-4} + B_6^6O_6^6 + B_6^{-6}O_6^{-6} \qquad (6)$$

as long as the Z′-axis is set perpendicular to the a-c mirror plane (i.e. parallel to the b axis). Although one of the principal efg axes must also align with the b-axis, the spatial orientation of the remaining two principal efg axes in the mirror plane is unknown. For each of the six possible sets of B_2^0 and B_2^2, an additional fit parameter, χ, was therefore needed to account for the angle of coordinate frame rotation about the b axis necessary to line up the efg principal axes and the CF theory axes in the mirror plane. This introduced the extra rank 2 CF parameter B_2^{-2} observed in (6) according to

$$(B_2^2)' = B_2^2\cos 2\chi \qquad \text{and} \qquad (B_2^{-2})' = -B_2^2\sin 2\chi \ . \qquad (7)$$

The best sets of CF parameters matched well with available optical spectroscopy and INS determinations of the lowest excited CF levels. They also led to useful predictions regarding low temperature induced Tm magnetisation.

4. Conclusion

This brief overview provides information in a user-friendly form designed to assist researchers endeavouring to exploit experimental efg results in an alternative frame of reference (i.e. a frame other than the conventional efg coordinate frame implicit in the asymmetry parameter condition that $0 \leq \eta \leq 1$).

References

[1] Rudowicz C 1985 *J. Phys. C* **18** 1415.
[2] Saensunon B, Stewart G A, Gubbens P C M, Hutchison W D and Buchsteiner A 2009 J.Phys.: Condens. Matter **21** 124215; 2010 J. Phys.: Condens. Matter **22** 029801.
[3] Stewart G A and Gubbens P C M 1999 J. Magn. Magn. Mater. **206** 17 - 26.